Journal of Photochemistry and Photobiology A: Chemistry 258 (2013) 17–29

Contents lists available at SciVerse ScienceDirect

Journal of Photochemistry and Photobiology A: Chemistry

journal homepage: www.elsevier.com/locate/jphotochem

Gas phase photocatalytic oxidation of decane at ppb levels: Removal kinetics, reaction intermediates and carbon mass balance

O. Debono[a,b,c], F. Thévenet[a,b,*], P. Gravejat[a,b], V. Héquet[c], C. Raillard[c], L. Le Coq[c], N. Locoge[a,b]

[a] Université Lille Nord-de-France, F-59000 Lille, France
[b] Ecole des Mines de Douai, d[pt] Chimie et Environnement, 941 rue Charles Bourseul, 59500 Douai, France
[c] L'UNAM, GEPEA UMR CNRS 6144, Ecole des Mines de Nantes, d[pt] Systèmes Energétiques et Environnement, 4 rue Alfred Kastler, BP 20722, F-44307 Nantes Cedex 3, France

ARTICLE INFO

Article history:
Received 3 October 2012
Received in revised form 18 February 2013
Accepted 23 February 2013
Available online 14 March 2013

Keywords:
Photocatalysis
Indoor air
VOC
Decane
Reaction intermediates
Carbon mass balance

ABSTRACT

This study focuses on the photocatalytic oxidation of decane at ppb levels, close to indoor air conditions. Although these concentrations are typical of indoor air volatile organic compound (VOC) levels, such conditions have been poorly investigated to date. Decane conversion rates higher than 90% were reached within 15 h for the highest initial concentration tested in the operating conditions used. Despite this high decane conversion, 18 reaction intermediates were detected in the gas phase. The main compounds, in terms of concentration level in the gas phase, were formaldehyde, acetaldehyde and propanal. The amounts of these compounds in the gas phase were linearly dependent on the initial decane concentration. A reaction pathway is proposed, based on reaction intermediate temporal profiles and the literature. It consists of six main steps describing the oxidation process from decane to CO and CO_2. The influence of the relative humidity level on the diversity and amounts of reaction intermediates was also studied. It was shown that moisture tends to shift the equilibrium of intermediates adsorption toward desorption, resulting in a relative increase in intermediate quantities in the gas phase. However, the monitoring of CO and CO_2 formation highlighted that, at the end of the reaction, a high mineralization rate could be obtained. Finally, an overview of the photocatalytic reaction is given through the carbon mass balance determined for various reaction advancements. This approach gives an overall evaluation of the photocatalytic process performance, from primary compound removal to reaction intermediate and mineralization.

1. Introduction

Indoor air quality is crucial for health since indoor air contamination triggers Sick Building Syndrome (SBS) or building-related illnesses [1]. Volatile organic compounds (VOCs) represent the major group of indoor air contaminants with total VOC concentrations ranging from 500 ppb to 1 ppm. Sources of VOCs are outdoor air, cooking, desks, carpets or ceiling emissions [2]. Several techniques, such as adsorption, non-thermal plasma or photocatalytic oxidation (PCO), can be used to remove them from the ambient air. In particular, PCO is a cost-effective method, both efficient and simple, which does not produce waste. It is therefore attractive for removing VOCs from indoor air. PCO potentially mineralizes VOCs into CO_2 and H_2O by Ultra-Violet (UV) irradiation of titanium dioxide (TiO_2) [3]. However, two points still have to be clarified:

(i) Before CO_2 formation, VOCs are oxidized step by step into reaction intermediates which could be less sensitive to photocatalytic oxidation, thus potentially forming organic by-products. This phenomenon has been observed during the PCO of a single compound and multi-component mixtures [4–6]. It thus appears necessary to perform temporal monitoring of the reaction intermediates in order to characterize the oxidation advancement and describe the reaction pathway.
(ii) The large majority of the studies performed on photocatalytic oxidation of VOCs are carried out at ppm levels whereas indoor air concentrations are approximately one thousand times lower (ppb level). In fact, the concentrations of the main indoor contaminants, i.e. alkanes, aromatic hydrocarbons and esters, rarely exceed 100 ppb [1]. Thus, an efficient investigation of PCO for indoor air treatment requires the photocatalytic reaction to be performed at ppb levels of VOCs in order to mimic the real indoor air conditions. The question of the transposition of the phenomena reported at the ppm range regarding primary

* Corresponding author at: Ecole des Mines de Douai, d[pt] Chimie et Environnement, 941 rue Bourseul, 59500 Douai, France. Tel.: +33 3 27 71 26 12; fax: +33 3 27 71 29 14.
E-mail addresses: debono_olivier@hotmail.com (O. Debono), frederic.thevenet@mines-douai.fr (F. Thévenet).

1010-6030/$ – see front matter © 2013 Elsevier B.V. All rights reserved.
http://dx.doi.org/10.1016/j.jphotochem.2013.02.022

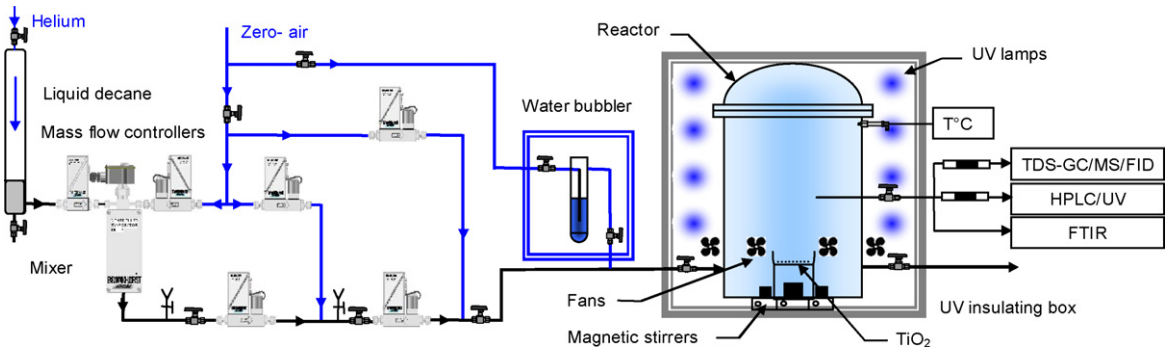

Fig. 1. General experimental set-up.

pollutant removal kinetics, reaction intermediate formation, and pollutant mineralization, is still being asked.

In order to answer these questions, this article focuses on the characterization of the photocatalytic degradation of decane in the ppb range. Our approach in a batch reactor enables: (i) the monitoring of decane removal profiles over the whole ppb range in order to investigate primary pollutant kinetics; (ii) the temporal monitoring of reaction intermediates produced during the oxidation of decane mineralization using appropriate analytical techniques; (iii) the determination of CO and CO_2 concentrations produced by the photocatalytic process in order to evaluate the ppb range carbon mass balance. A similar approach was previously used to characterize toluene photocatalytic reactivity in the ppb range [4]. These two compounds are complementary because of their different chemical structures and reactivity.

Decane can be considered one of the major alkanes monitored in indoor air. Its concentration can reach 50 ppb. For example, in North America, decane mean and maximum concentrations are 0.44 and 13 ppb, respectively, in existing residences and 3.9 and 22 ppb in new single-family houses [7]. Similarly, Tanaka-Kagawa et al. have determined 1 and 43 ppb as the mean and maximum concentrations of decane in 50 residences in Japan [8]. Likewise, in a Spanish dwelling where the inhabitants were affected by SBS symptoms, Gallego et al. [1] measured between 0.25 and 3.4 ppb of decane. In addition, heptane has been recommended as a reference pollutant for PCO systems evaluations in the XP B44-013 French standard [9]. Consequently, long-chain alkanes, and more especially decane, are model pollutants of interest for indoor air treatment.

Decane is expected to produce a large diversity of reaction intermediates and by-products using the PCO technique. However, only a few studies have been dedicated to decane [10–12] or alkanes PCO [5,6,13–17]. Moreover, these investigations have generally been carried out at the ppm level and reaction intermediates have not been clearly identified.

This paper focuses on the photocatalytic degradation of decane at the ppb level. Firstly, the removal kinetics of decane are investigated over the whole ppb range. Next, the diversity and the amounts of the reaction intermediates during decane PCO are presented; a reaction pathway is proposed and discussed. Then, the influence of initial decane concentration and relative humidity on reaction intermediates is reported. Finally, by determining decane mineralization, a carbon mass balance of the photocatalytic oxidation of decane is established.

2. Experimental

The experimental set-up can be divided into three parts: (i) a ppb level VOC generation system, (ii) a 120 L Pyrex photocatalytic reaction chamber, and (iii) analytical systems for gas phase characterization at ppb levels. This device was described in detail in a previous paper [4] and a general diagram is presented in Fig. 1.

Air used for all experiments was supplied by a zero-air generator (Claind AZ 2020) coupled with a PSA (Pressure Swing Absorption) air purifying system. The first step to obtain pure air consisted in mineralizing organic compounds present in the 6-bar compressed air using a thermal catalytic treatment unit. At the outlet of the first step, the level of total VOCs in the gas stream was lower than 10 ppt. The second step consisted in removing CO, CO_2 and moisture from the gas stream by sequential absorption under 5 bar. At the outlet of the second step, less than 10 ppb of CO_2, 80 ppb of CO and 10 ppm H_2O were monitored in the gas stream using Infrared Fourier Transform spectroscopy (Section 2.3). The obtained air is called zero-air.

2.1. VOC generation system

In order to generate accurate concentrations of decane in air from 1 to 1000 ppb, an appropriate VOC generator system was developed. First, 300 mL of liquid decane supplied by Aldrich was placed in a stainless steel pressurized 1 L tank. The pressure of helium in the tank ranged from 1.1 to 1.3 bar. The liquid VOC flow was regulated from 0 to 200 mg h^{-1} using a Bronkhorst liquid mass flow controller downstream of the tank. The liquid VOC was vaporized and mixed with zero-air in the Bronkhorst CEM system. The gas stream obtained was sampled and diluted with zero-air twice with appropriate ratios in order to reach the target concentrations. At the outlet of the generation system, the concentration of decane could be tuned from 1 to 1000 ppb with an accuracy of 20%. Since moisture was lower than 10 ppm, this gas stream was used directly for experiments under dry air conditions. In order to work with 50% relative humidity (RH), the air stream containing decane was mixed with an equivalent zero-air flow previously humidified (wet conditions). Humidity level was checked with a Testo hygrometer characterized by an uncertainty of 2%.

2.2. Photocatalytic reaction chamber

Since the purpose of this study was to investigate the photocatalytic oxidation of decane at each step of the reaction advancement, a large volume batch reactor was selected. This approach enabled the temporal profile of each species formed and consumed by the reaction to be characterized. The photocatalytic reaction chamber consisted of a 120 L Pyrex reactor, which could be kept in the dark or illuminated by nine PL-L-40 Philips UV-lamps. The emission band of the lamp in the UV range was centered on 365 nm. No wavelengths lower than 350 nm were emitted. The resulting UV photon flux was characterized using a SolaCheck photoradiometer at 70 different points of the reaction chamber. The photon flux was homogeneous in the chamber with an average of 10 ± 1 mW cm^{-2}. In order to

Table 1
TDS-GC analytical parameters under dry air conditions.

TDS parameters	Initial temperature (°C)	10
	Temperature ramp (°C min^{-1})	50
	Final temperature (°C)	250
	Final time (min)	10
	Flow rate (mL min^{-1})	50
Refocusing on CIS and injection in GC	Initial temperature (°C)	−100
	Temperature ramp (°C s^{-1})	12
	Final temperature (°C)	250
	Final time (min)	10
Elution on chromatographic column	Initial temperature (°C)	0
	Initial time (min)	4
	Temperature ramp (°C min^{-1})	15
	Final temperature (°C)	250
	Flow rate (mL min^{-1})	4

ensure the experiment's reproducibility, the reaction chamber was swept with wet zero-air for 12 h under UV illumination before each experiment. The photocatalyst used for all experiments was 100 mg of P25-Degussa TiO_2 powder dispersed in the lower part of the reaction chamber. In this study, the photocatalyst was used in powder form in order to isolate the interactions between the VOCs and TiO_2 and to overcome the effect of the TiO_2 support.

After cleaning the photocatalyst and the reaction chamber with wet zero-air and UV irradiation, the system was swept in the dark for 14 h with an air flow containing the target amount of decane in order to reach the VOC adsorption equilibrium in the reactor. Then, the chamber was closed and the decane concentration was monitored twice. Preliminary static experiments performed in the dark for 48 h with 800 ppb of toluene had shown that, once the chamber was closed, the VOC concentration decrease was less than 5% over 24 h. The beginning of UV irradiation defined $t = 0$ for each photocatalytic experiment. Then, the gas phase was characterized during the whole photocatalytic process.

2.3. Gas phase sampling and analytical devices

Three main analytical devices were used for a complete gas phase characterization: (i) Gas Chromatography (GC) for VOCs, (ii) derivatization and Liquid Chromatography (HPLC) for carbonyls, and more especially formaldehyde, and (iii) Infrared Fourier Transform (FTIR) spectrometry for CO and CO_2.

In order not to modify significantly the volume inside the batch reactor during the photocatalytic process, less than 10% of the total volume (i.e. 12 L) was sampled for analytical purposes. For each GC analysis, 1000 mL of gas was sampled by the Gerstel Thermal Desorption System (TDS) with a constant flow rate of 100 mL min^{-1}. The sample was first trapped on a multi-sorbent cartridge (CarboSieve SIII + CarboPack B + CarboPack C), then refocused at −100 °C on a CarboPack B filled trap called a Cooled Injection System (CIS). The GC was equipped with an Agilent DB-5MS capillary column (60 m × 0.32 mm × 1 μm). Using a calibrated Y-shaped restriction, the column was connected to two detectors: (i) a Flame Ionization Detector (FID) for compound quantification and (ii) a Mass Spectrometer (MS) for compound identification. Simultaneous detection was performed at the column outlet. Analytical TDS-GC parameters corresponding to dry air analyses are listed in Table 1. For wet air (50% RH) analyses, CarboSieve SIII was replaced by CarboPack X in order to prevent water trapping during sampling. Irrespective of the dry or wet conditions, detection limits were lower than 100 ppt for each VOC monitored in this study. Calibrations of the monitored compounds were performed by loading the sampling multi-sorbent cartridges with various known amounts of VOC obtained from a certified gas cylinder or vaporized liquid VOC.

The chromatographic technique enabled a wide diversity of VOCs to be monitored, but not formaldehyde. Since this is a key compound for indoor air quality and is expected to be a major by-product, a complementary analytical technique was used. 1000 mL of gas was sampled from the reaction chamber through Waters silica cartridges impregnated with 2,4-dinitrophenylhydrazine (DNPH) [18]. This reactive sampling enabled light carbonyl derivatization on the cartridges. These were then eluted and analyzed by HPLC as described in detail by Coddeville et al. [19]. With this method, the quantification limit of formaldehyde is 10 ppb. Measurement of acetaldehyde was performed simultaneously with this HPLC method and with GC in order to crosscheck the quantifications, which differed by only 15%.

The detection and quantification of CO and CO_2 was performed using a Thermo-Electron high resolution Fourier Transform Infrared Spectrometer (FTIR) Antaris IGS equipped with a heated 10 m optical-path length cell and an MCT (Mercury Cadmium Telluride) detector. The level of CO_2 in ambient air usually ranges from 350 to 400 ppm. This is much higher than the expected formation of CO_2 due to the photocatalytic mineralization of decane. The highest concentration of decane in the experiment was 800 ppb. Assuming that decane mineralization can be achieved, the highest CO_2 concentration expected in the reaction chamber would remain below 8 ppm. This value is dramatically small in comparison to ambient air CO_2 concentration. Thus, the PSA system was necessary to remove CO_2 from the supplied air. The CO_2-free zero-air stream (less than 10 ppb) was simultaneously used to feed the VOC generator and to purge the FTIR optical device.

FTIR spectra were collected using Result-3 software with 6 scans per spectrum and a spectral resolution of 0.5 cm^{-1}. The fundamental asymmetric stretch vibration of CO_2 in the region 2388–2383 cm^{-1} was selected for quantification. To avoid the overlapping region of absorption signals for CO and H_2O, the quantification of CO was carried out using the average of four rotational absorption peaks associated with the C—O stretch vibration. The R(4), R(5), R(6) and R(7) peaks, 2163.5–2160.1 cm^{-1}, 2167.4–2163.7 cm^{-1}, 2170.7–2167.1 cm^{-1} and 2173.1–2171.9 cm^{-1} respectively, were selected. Calibration curves for CO and CO_2 were determined by passing 1 L min^{-1} of standard gases provided and certified by Praxair through the gas-cell. Calibration concentrations were adjusted from 240 ppb to 10 ppm. 500 scans were taken per standard spectrum. For calibration curves and quantitative data processing, TQ-Analyst-8 software was used. The detection limits were evaluated as twice the Signal/Noise ratio in the region of interest and were 10 ppb and 76 ppb for CO_2 and CO, respectively.

3. Results and discussion

3.1. Decane removal

The photocatalytic oxidation of decane was carried out for various initial concentrations ranging from 30 to 810 ppb under wet and dry air conditions. No photocatalyst deactivation was noticed during all the experiments but the photocatalyst surface was regenerated between each experiment to ensure the same chemical surface state throughout the study. The profiles of decane concentration as a function of irradiation time under both dry and wet air are presented in Fig. 2. It can be seen that the complete conversion of decane can be achieved at ppb range in a static regime over the observation period. Moreover, the decrease in decane concentration is characterized by mono-exponential decay profiles under both dry and wet air.

Each decane degradation curve presented in Fig. 2 can be modeled by an apparent first order kinetic rate law. For this

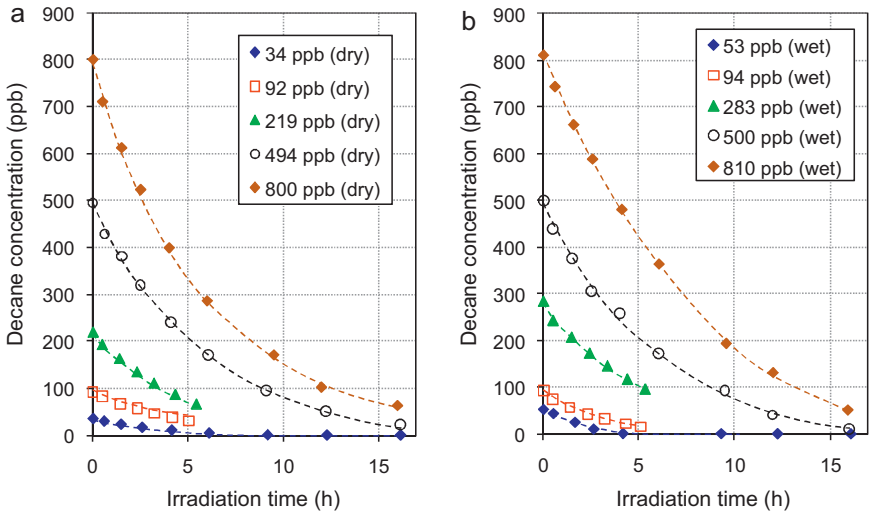

Fig. 2. Change in decane concentration as a function of irradiation time during photocatalytic oxidation (a) under dry air and (b) under wet air (RH = 50%) for various initial concentrations of decane.

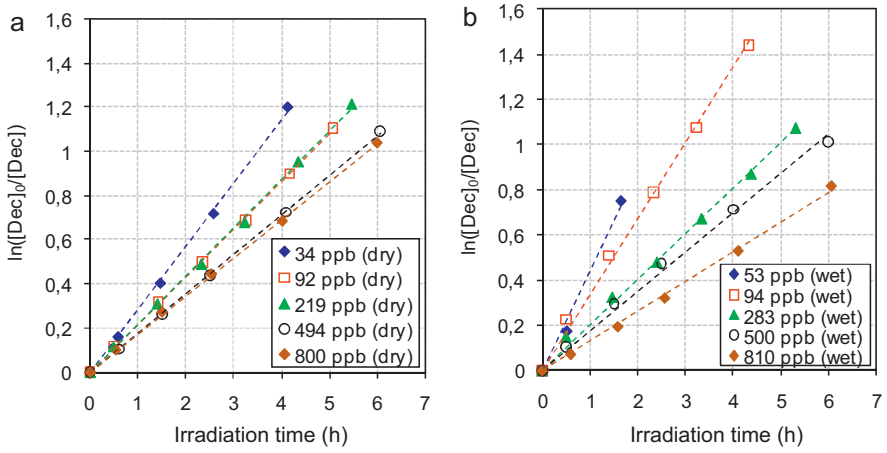

Fig. 3. Change in $\ln([Dec]_0/[Dec])$ as a function of irradiation time during the photocatalytic degradation of decane (a) under dry air and (b) under wet air (RH = 50%), C_0^{dec} = 34–810 ppb.

reason, the first step was to express the decane reaction rate r by the following equation (Eq. (1)), where k is the reaction constant, $[Dec]$ the concentration of decane and n the reaction order.

$$r = k \cdot [Dec]^n \quad (1)$$

By plotting $\ln(r)$ versus $\ln([Dec])$, it was shown that all kinetics can be represented by a first order reaction rate. To compare the associated kinetic constants obtained for each degradation curve, the reaction order n was fixed at 1 and the rate constants k were calculated by determining the slopes of the straight lines $\ln([Dec]_0/[Dec]) = f(t)$ presented in Fig. 3. It can be seen here that the slopes, i.e. k values, depend on initial decane concentration.

The values of k calculated for each experiment, along with their standard errors, are listed in Table 2. They range from 0.173 to 0.286 under dry air and from 0.132 to 0.440 under wet air. They are plotted as a function of initial decane concentration in Fig. 4.

Values of k tend to increase significantly with decreasing initial decane concentration, under both dry and wet air. A similar trend between initial rate and initial concentration has already been reported by numerous authors [20–23]. It is well described by the Langmuir–Hinshelwood law, which takes into account in the kinetic models several steps of the mechanism, including the adsorption of the molecules onto the catalyst surface. The fact that

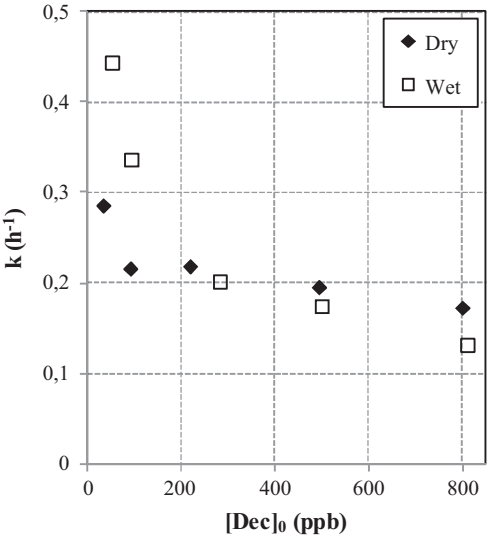

Fig. 4. Change in k as a function of initial concentration of decane $[Dec]_0$ during the photocatalytic degradation of decane considering a first order reaction (n = 1), under dry and wet (RH = 50%) conditions.

Table 2
Reaction constants of the photocatalytic oxidation of decane, considering a first order reaction ($n = 1$), $C_0^{dec} = 34–810$ ppb; RH = 0 or 50%.

Dry air		Wet air	
$[Dec]_0$ (ppb)	k (h^{-1})	$[Dec]_0$ (ppb)	k (h^{-1})
34	0.286 ± 0.003	53	0.440 ± 0.020
92	0.216 ± 0.001	94	0.340 ± 0.010
219	0.219 ± 0.002	283	0.202 ± 0.003
494	0.196 ± 0.003	500	0.175 ± 0.004
800	0.173 ± 0.001	810	0.132 ± 0.002
Average of coefficients ± standard deviation	0.22 ± 0.04	Average of coefficients ± standard deviation	0.26 ± 0.13

the apparent kinetic constants are not constant according to the initial concentrations also means that this is an approximation to model each degradation rate by a first order reaction rate. In fact, the corresponding mechanisms are more complex. However, in this work, the objective was first to assess the formation and degradation of reaction intermediates so efforts were focused on this and the kinetic modeling was not investigated further.

Moreover, the rise of k was higher under wet air at concentrations lower than 100 ppb. This can be explained by the influence of the water molecules on the different steps of the mechanism [20,21].

The influence of humidity on the degradation rate has been studied for different alkanes in the past but no general trend can be extracted from those studies [13]. However, it seems that water vapor can have two opposing effects: (i) promotion of the degradation by the formation of hydroxyl radicals [24] and (ii) at higher humidity, inhibition of the degradation by competition with VOCs for adsorption onto the active sites of TiO_2. When varying humidity, several studies have shown that both effects can be predominant, depending on the humidity; other studies have reported that only one of these effects is visible. For example, Twesme et al. [6] showed that the degradation rates of several alkanes reach their maximum at a relative humidity of 40% under 70 °C. Below 40%, promotion by hydroxyl radicals is predominant whereas above 40% inhibition by competition for adsorption becomes predominant. Zhang and Liu [17] also determined an optimum at a relative humidity of 20% under 21 °C with hexane. On the contrary, Shang et al. [16] demonstrated a continuous decrease in the degradation rate of heptane when the relative humidity was increased from 0% to 60%. This result was also obtained by Boulamanti and Philippopoulos [13] who reported a similar trend for several C_5–C_7 alkanes with water vapor concentrations ranging from 0 to 37,000 ppm. These contradictory effects of humidity on alkane degradation rates may be attributed to the various experimental conditions used in degradation tests: concentration levels of alkanes, continuous or discontinuous VOC supply to the reactor, temperature, RH range investigated. Looking at the kinetic constants obtained for decane, it seems that water vapor, via hydroxyl radicals, has a promoting effect on PCO at concentrations lower than 100 ppb. This is encouraging because it corresponds to real indoor air treatment conditions.

3.2. Reaction intermediates

Simultaneously with the study of decane degradation, reaction intermediate formation and removal were monitored by appropriate analytical procedures. During the photocatalytic degradation of decane under wet air, 18 reaction intermediates were identified in the gas phase. These compounds are listed in Table 3 and classified according to their chemical nature. Three different decanones and three different decenes were identified. However, as the position of the unsaturation within these compounds was not precisely determined, they are gathered under the names x-decenes and x-decanones in Table 3. The majority of the intermediates identified were carbonyl compounds and alcohols. Djeghri et al. [14] and Shang et al. [16] have also detected these kinds of major compounds during the photocatalytic degradation of other lighter, linear or branched alkanes, with initial concentrations higher than one ppm.

The temporal changes in reaction intermediates are represented in Fig. 5 for an initial decane concentration of 810 ppb in the presence of wet air (50% RH). Hexanal, octanal, 1-propanol and isopropanol were detected but their profiles are not represented because their concentrations were lower than the quantification limit of the analytical system. In addition, x-decanones and x-decenes were not calibrated thus their profiles were plotted using the areas of their chromatographic FID peaks.

The temporal profiles of the intermediates consist of three phases: (i) intermediate formation, (ii) reaching a maximum concentration (t_{MAX}), and (iii) decrease in the intermediate concentration. The irradiation time (t_{MAX}) corresponding to the maximum concentration is reported in Table 3 for each intermediate. This time increases almost linearly as the number of carbons in the compound decreases. This is consistent with the advancement of the degradation reaction. In the case of intermediates with the highest number of carbon atoms, such as heptanal or x-decanones, the maximum concentrations are reached before 5 h of irradiation. On the contrary, for formaldehyde, the removal step begins only after 14 h of irradiation. Most of the quantified intermediates require more than 20 h to be completely removed from the gas phase, whereas decane is completely removed at this irradiation time. Moreover, after 25 h of irradiation, some intermediates such as acetaldehyde or acetone are still not completely removed. In order to explain the delay in the photocatalytic degradation of

Table 3
List of the reaction intermediates identified in the gas phase during photocatalytic decane degradation. For each compound, "t_{MAX}" corresponds to the temporal position of the maximum concentration during the photocatalytic degradation of 800 ppb of decane under 50% RH.

Aldehydes	t_{MAX} (h)	Ketones	t_{MAX} (h)	Alcohols	t_{MAX} (h)	Others	t_{MAX} (h)
Formaldehyde	>13.7	Acetone	12	Ethanol	9.6	Methyl acetate	12
Acetaldehyde	9.6	2-Butanone	9.6	1-Propanol	(Not determined)	x-Decenes	2.3
Propanal	9.6	Methylvinylketone	6.1	Isopropanol	(Not determined)		
Acroleine	9.6	x-Decanones	4.3				
Butanal	6.1						
Pentanal	6.1						
Hexanal	6.1						
Heptanal	4.1						
Octanal	∅						

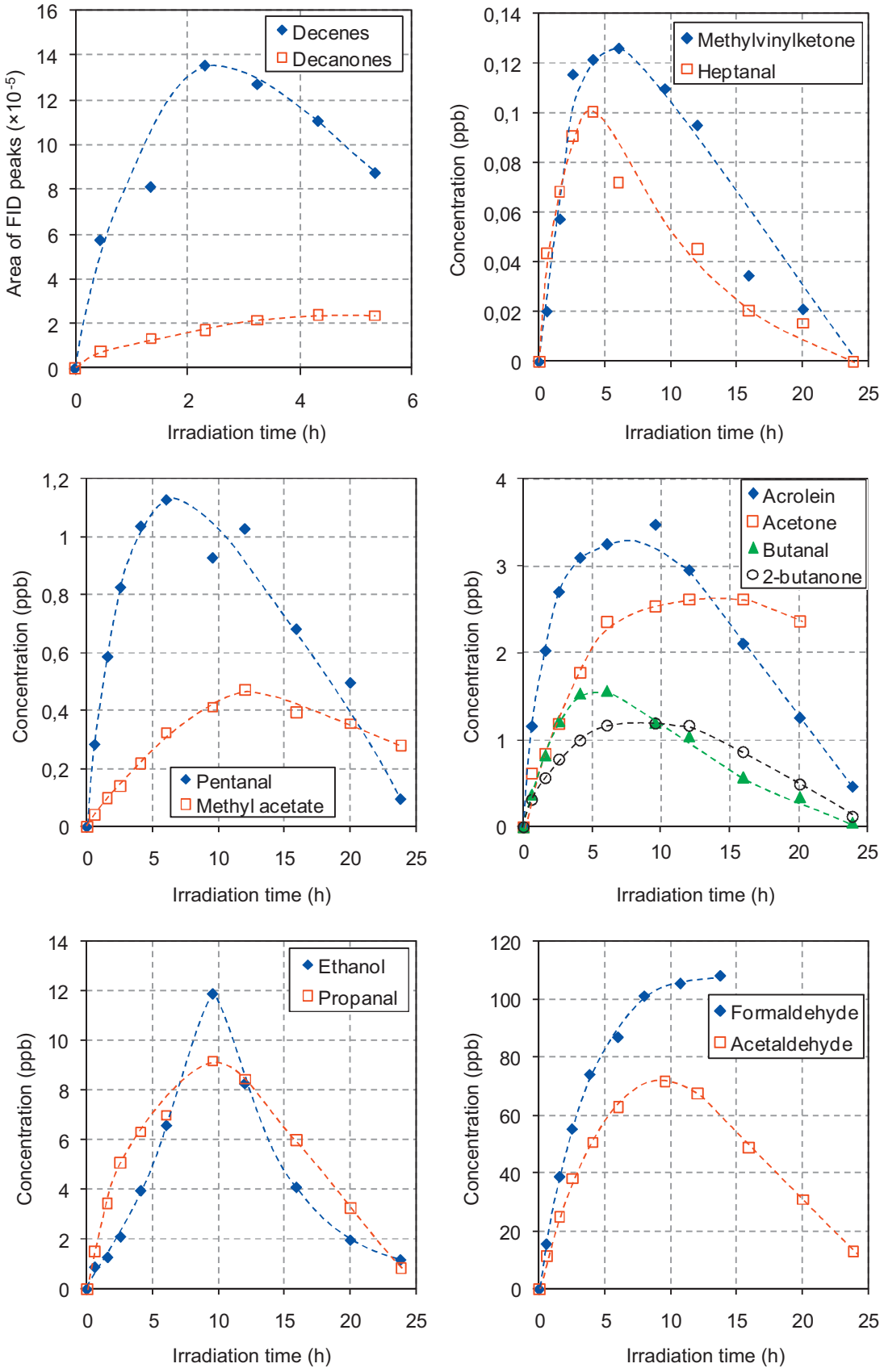

Fig. 5. Temporal changes in reaction intermediate amounts during the degradation of decane, $C_0^{dec} = 810$ ppb; HR = 50%.

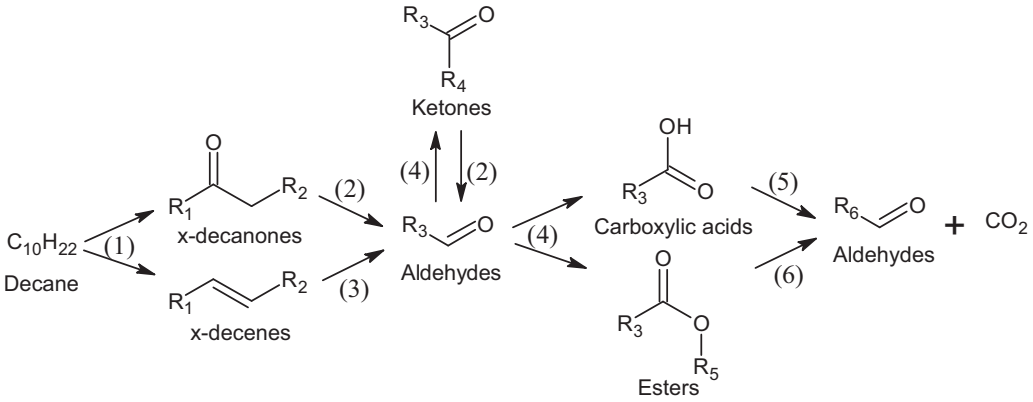

Fig. 6. General scheme of the reaction pathway of decane PCO (50% RH) (R_1, R_2, R_3, R_4 and R_5: alkyl roots).

these light intermediates, the following hypothesis can be proposed: after the complete removal of decane and high molecular weight reaction intermediates from the gas phase, some strongly adsorbed reaction intermediates may remain on the TiO_2 surface and be slowly oxidized into lower molecular weight compounds such as formaldehyde or acetaldehyde. This point will be clarified later in this paper (i) by investigating a reaction pathway based on previous studies and on the experimental results of the present study and (ii) through the analysis of the carbon mass balance of the reaction for different advancements of the oxidation process.

3.3. Reaction pathway

Photocatalytic oxidation is initiated by the production of electron/hole pairs under UV irradiation. The majority of the holes and electrons recombine but a fraction reaches the TiO_2 surface. Here, electrons and holes may react either with adsorbed VOCs, so-called direct reactivity, or with water and oxygen which leads to the formation of surface-stabilized oxidizing species such as OH radicals and superoxide radicals that further react with decane, so-called indirect reactivity. No PCO reaction pathway has been proposed for decane to date. Based on the nature and the ordering of the reaction intermediates monitored and on the literature associated with alkanes PCO, a reaction pathway for decane photocatalytic oxidation under wet air (50% RH) is proposed and depicted in Fig. 6. It can be divided into six main steps, which are justified and detailed in the following.

- Step 1

  Several previous studies [5,14–16] have reported that alkane PCO begins by the abstraction of a hydrogen atom from a carbon atom by a hydroxyl radical. More precisely, Djeghri et al. [14] have shown that the oxidation of alkane carbons proceeds in a particular order: $C_{tert} > C_{quat} > C_{sec} > C_{prim}$. As a result, considering linear alkanes like decane, secondary carbons are attacked rather than primary ones. After hydrogen abstraction by hydroxyl radicals, alkyl radicals are formed, pending electrons being located on a secondary carbon of the alkyl chain. Then, alkyl radicals undergo the addition of hydroxyl radicals and are converted into secondary alcohols. As reported by Shang et al. [16], alcohols rapidly react under PCO so they are hardly detected. According to Djeghri et al. and Peral and Ollis [14,25], alcohols can undergo two reactions: (i) dehydration into alkenes and (ii) oxidation into ketones. Thus, step 1 leads to the formation of alkenes and ketones containing the same number of carbons as the primary pollutant. Indeed, Shang et al. [16] have reported that heptane first produces 3-heptanone, 4-heptanone and 3-heptene. Likewise, Hägglund et al. [15] have identified acetone during propane PCO. Similarly, for C_2–C_8 alkanes, Djeghri et al. [14] have noted the formation of not only the corresponding ketones but also, in smaller quantities, alcohols with the same number of carbon atoms as the original alkane.

  The fact that decenes and decanones are the reaction intermediates characterized by the shortest t_{MAX} is coherent with the reaction pathway proposed for step 1 and described in Fig. 7. Moreover, the absence of decanal during decane PCO supports the fact that the secondary carbon atoms of the alkyl chain are the most reactive. In addition, the fact that decanols were not monitored supports the hypothesis of a high reactivity for these compounds. Nevertheless, the position of the maximum concentration for decenes is lower than for decanones. This could be explained by a higher reaction rate for decene oxidation.
- Step 2

  Step 2 corresponds to decanone degradation. Among ketones, acetone and 2-butanone PCO have been the most frequently studied in the last decade [20–22,25–34]. For instance, Raillard et al. [22] identified acetaldehyde as the main intermediate of 2-butanone oxidation. They also detected methyl formate. On the basis of the pathways previously proposed by Henderson [28,33] for 2-butanone and acetone, decanones could be adsorbed

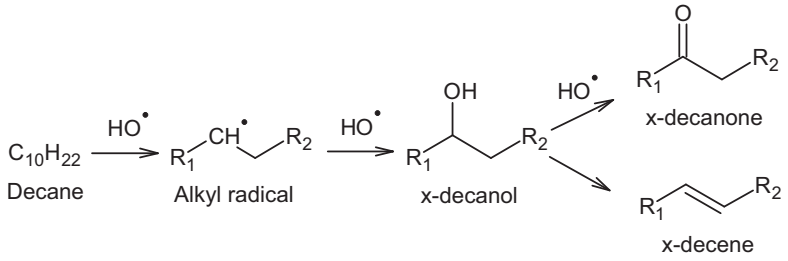

Fig. 7. Step 1 of the reaction pathway of decane PCO: formation of x-decanone and x-decene (R_1 and R_2: alkyl roots).

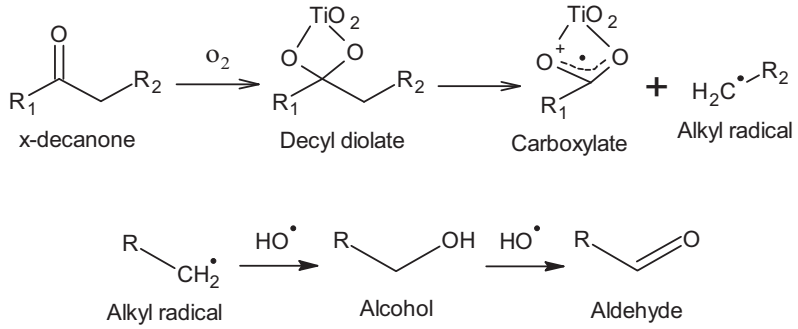

Fig. 8. Step 2 of the reaction pathway of decane PCO: (a) dissociative adsorption of x-decanone into a carboxylate and an alkyl radical; (b) formation of alcohols and aldehydes from alkyl radicals (R_1, R_2 and R: alkyl root).

dissociatively onto TiO_2, reacting with adsorbed O_2. The so-formed ketone diolates suggested by Henderson [28] would complex onto the TiO_2 surface. This unstable complex would easily dissociate into an alkyl radical and a carboxylate stabilized on TiO_2 (Fig. 8a). The carboxylate is more stable than the ketone diolate specie so it is less likely to decompose. However, several authors have previously reported the decomposition of formate, a carboxylate, into CO and CO_2 [24,25]. One possibility for the degradation of carboxylates containing more than one carbon atom is that alkyl radicals could be formed on the top of the chain. Another possibility is that they react with an alkyl radical to form esters, explaining the production of methyl formate during 2-butanone PCO [22]. This approach would explain the production of methyl acetate during decane PCO. Decanones would lead to the formation of various alkyl radicals containing a maximum of eight carbon atoms. These alkyl radicals would be rapidly oxidized into alcohols and then into aldehydes [35] (Fig. 8b). As a consequence, decanone degradation would be one source of the low molecular weight alcohols (isopropanol, 1-propanol and ethanol) and aldehydes (from formaldehyde to octanal). It can be seen that the detected alcohols contain a maximum of 3 carbon atoms in their structure. Longer alcohols are probably also formed but, as reported by Shang et al. [16], the photocatalytic oxidation of this class of compounds into corresponding carbonyls is characterized by high reaction rates. As a result, they could not be detected under our analytical conditions since the first monitoring of the gas phase occurred after 30 min of reaction and the following analyses were separated by at least 1 h. Moreover, long-chain alcohols probably stay adsorbed on TiO_2 and are rapidly oxidized. This is consistent with our observation of reaction intermediates in that: (i) nonanal was not detected in the gas phase, but (ii) all linear aldehydes, from C1 to C8, were quantified; (iii) only low molecular weight alcohols, mainly ethanol, were monitored.

- Step 3

  Step 3 corresponds to decenes degradation. Previously, Shang et al. [16] proposed that 3-heptene could be oxidized into propanal and butanal. The double bond in alkenes would be attacked. However, Ohno et al. [36] reported the formation of 2-decanone, 1,2-epoxidecane and decanal during the photocatalytic oxidation of 1-decene in water. Although several pathways could be considered, those evidenced in water cannot be transposed to air. Moreover, the fact that we monitored aldehydes containing from 1 to 8 carbon atoms clearly supports the pathway suggested by Shang et al. [16] (Fig. 9).

- Step 4

  Step 4 consists of the oxidation of aldehydes. Several authors have shown that aldehydes are oxidized into carboxylic acids [25,37–39]. However, carboxylic acids were not detected in the gas phase during decane PCO at the ppb level. As reported by Méndez-Roman and Cardona-Martinez [40] investigating surface species during toluene PCO, compared to toluene, benzaldehyde and benzyl alcohol, benzoic acid is poorly desorbed from the photocatalyst and is responsible for its deactivation. This was confirmed by Deveau et al. [41] who reported energy of desorption values of 88, 123 and 140 kJ mol^{-1} for toluene, benzaldehyde and benzoic acid, respectively. More generally, compared to alkanes and aldehydes, the corresponding carboxylic acids are characterized by a higher energy of desorption. The desorption step being hindered, carboxylic acids are produced, but poorly observed in the gas phase.

  Another reaction pathway for aldehydes was reported by Kominami et al. [42]. These authors observed the formation of methyl formate during methanol PCO, which they supposed came from the recombination of intermediates, particularly from the dimerization of formaldehyde. Thus, they considered aldehydes as a possible source of esters.

  Blount et al. identified acetone during acetaldehyde PCO [43] and Mo et al. during toluene PCO [44]. The pathway that Mo et al. proposed for the formation of acetone was a reaction between a carbonyl radical and a methyl radical. So, aldehydes can also be sources of ketones, here acetone and 2-butanone. The next step of ketone degradation is similar to the pathway of decanone degradation (step 2).

  Fig. 10 represents the three possible pathways for aldehyde PCO. The principal one would be oxidation into carboxylic acid because of the reactivity and the concentration of the hydroxyl radicals related to the aldehydes and the alkyl radicals.

- Step 5

  Step 5 concerns the degradation of carboxylic acids. According to the photo-Kolbe process [45], carboxylic acids lose their carboxyl group to form alkyl radicals (Fig. 11). These are subsequently oxidized to aldehydes, as previously described in step 4 (Fig. 10). Finally, as reported by Boulamanti et al. and Raillard et al. [13,20,21], the advancement of the oxidation reaction corresponds to shorter and shorter alcohols, aldehydes and acids until mineralization. This cyclic pathway is coherent with our observations; in the case of the major reaction intermediates, aldehydes, the smaller the number of carbons, the later the maximum is reached and the more the concentration increases.

- Step 6

  Step 6 describes the degradation of esters. As seen in step 2, several authors have proposed a reaction pathway for methyl formate PCO [24,25]. Methyl formate would be adsorbed

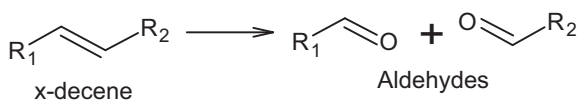

Fig. 9. Step 3 of the reaction pathway of decane PCO: dissociation of x-decene into aldehydes from the pathway proposed by Shang et al. [16] (R_1 and R_2: alkyl roots).

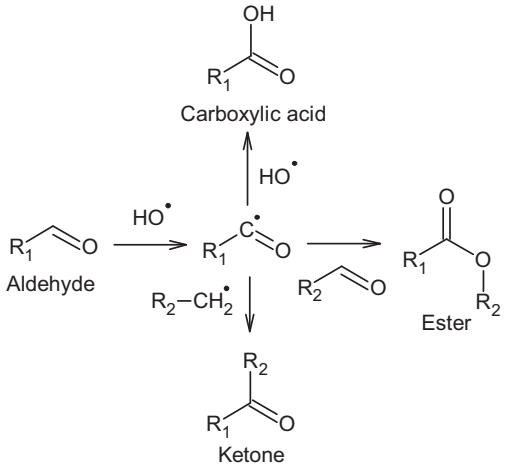

Fig. 10. Step 4 of the reaction pathway of decane PCO: aldehyde behavior; oxidation into carboxylic acid or formation of ester or ketone (R_1 and R_2: alkyl roots).

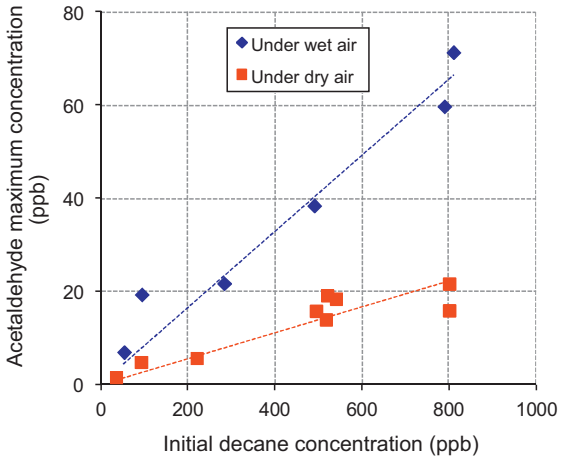

Fig. 14. Maximum acetaldehyde concentration versus initial decane concentration (squares: dry conditions; diamonds: wet conditions (50% RH)).

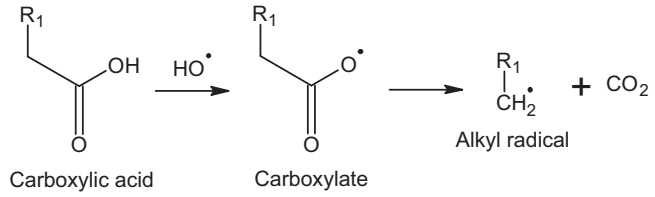

Fig. 11. Step 5 of the reaction pathway of decane PCO: decarboxylation of carboxylic acids by the photo-Kolbe process and formation of alkyl radicals (R_1: alkyl root).

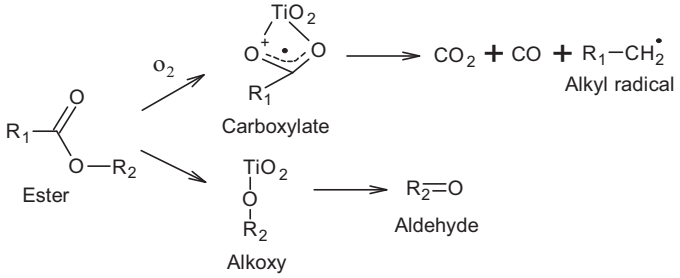

Fig. 12. Step 6 of the reaction pathway of decane PCO: dissociative and reactive adsorption of esters onto the TiO_2 surface into alkyl radicals and aldehydes (R_1 and R_2: alkyl roots).

dissociatively onto TiO_2 as methoxy and formate radicals. Formate radicals lead to the formation of CO and CO_2 whereas methoxy produces formaldehyde. Thus, more generally, esters would be transformed into carboxylates and alkoxys and then into aldehydes, CO and CO_2. Methyl acetate and ethyl acetate could form an acetate radical. Then, one possibility is that this radical gives CO, CO_2 and a methyl radical. This step of the reaction pathway is depicted in Fig. 12.

Two quantified reaction intermediates, acrolein and methylvinylketone, are not included in the reaction pathway. They have already been identified as by-products of toluene PCO [3,44]. However, their origins were not discussed. Their formation could be the result of primary alcohols dehydration into alkenes. As represented in Fig. 13, these alkenes would then be oxidized into enals, such as acrolein, or enones, such as methylvinylketone.

The reaction pathway proposed in Section 3.3 is based on the reaction intermediates identified under wet air conditions and for an initial decane concentration of 810 ppb. Experiments carried out with different initial decane concentrations and/or with dry air led to our questioning the proposed reaction pathway and the amounts of reaction intermediates regarding the influence of these parameters.

3.4. Influence of initial decane concentration and relative humidity on reaction intermediates

3.4.1. Influence of initial decane concentration

The influence of the initial decane concentration on intermediate quantities was investigated in the ppb range. By increasing the initial decane concentration from 50 ppb to 800 ppb, three observations can be reported:

(i) The same diversity of reaction intermediates was found in the gas phase, suggesting the reaction pathway is not modified when changing the initial concentration of pollutant in the ppb range.
(ii) The ordering of the intermediate temporal profiles was not significantly modified. Only the duration of complete intermediate degradation was diminished by decreasing the initial decane concentration from 800 to 50 ppb. Thus, the initial decane concentration only affects the irradiation time necessary to eliminate the reaction intermediates.
(iii) Finally, the amounts of reaction intermediates in the gas phase increased along with the initial decane concentration. This behavior is illustrated in Fig. 14 with acetaldehyde: the maximum concentration of acetaldehyde measured in the gas phase is plotted versus initial decane concentration for dry and wet air conditions. According to Fig. 14, linear relations are obtained for acetaldehyde as an intermediate product of

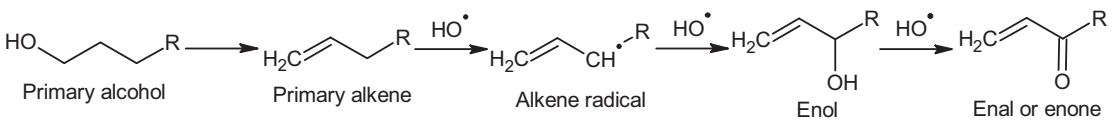

Fig. 13. Reaction pathway of acrolein and methylvinylketone formation during decane PCO (R: alkyl root).

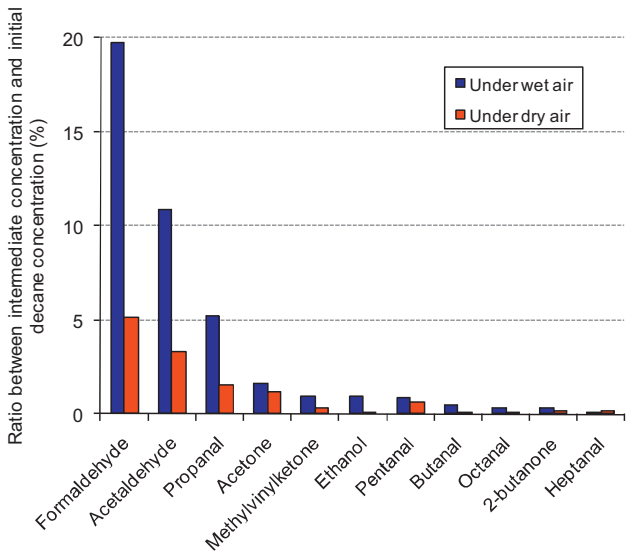

Fig. 15. Averages of ratios between intermediate maximum concentration and initial decane concentrations for several reaction intermediates under wet air (RH = 50%) and under dry air.

decane PCO with 80% and 94% confidence for dry and wet air, respectively. This linear trend is also observed for formaldehyde and propanal.

These results confirm that the reaction pathway is not modified when the initial pollutant concentration is changed at the ppb level.

3.4.2. Influence of relative humidity

In order to assess the influence of relative humidity on the formation of gaseous intermediates during decane PCO, experiments were carried out at two levels of water vapor content: 0% RH and 50% RH. It was found that wet air (i) triggers a delay in intermediate elimination and (ii) significantly modifies intermediate quantities. To compare these quantities, for each experiment and each compound, the ratios of intermediate maximum concentration to initial decane concentration were calculated. The averages for all initial concentrations of the ratios obtained are reported in Fig. 15.

As presented in Fig. 14 for acetaldehyde, the same trend is observed for all reaction intermediates: ratios are higher with wet air than with dry air for all initial concentrations. This shows that water vapor induces a significant increase in the quantities of reaction intermediates in the gas phase. In the literature, it is reported that water vapor can have two effects on photocatalytic oxidation: (i) promotion of VOC degradation by hydroxyl radicals and (ii) inhibition of VOC degradation by competitive adsorption between water and VOCs. Decane conversion does not seem to be affected by these effects, whereas quantities of reaction intermediates in the gas phase are increased by the presence of water vapor. Two hypotheses, based on the literature, can explain this behavior: (i) under wet air, hydroxyl radicals may enhance the degradation of intermediates toward mineralization, which could increase their quantities in the gas phase; (ii) water vapor competes with reaction intermediates for adsorption onto TiO_2. As a result, under wet air, reaction intermediates desorb from the TiO_2 surface so that their gas phase concentrations increase. This second hypothesis is supported by Twesme et al. [6] at the ppm level. During isobutane and propane elimination, the gas phase concentration of acetone rose significantly when the relative humidity was increased whereas their conversions were not modified. They also observed that water vapor inhibited the mineralization of the VOCs. According to our results, both hypotheses are possible. Decane mineralization,

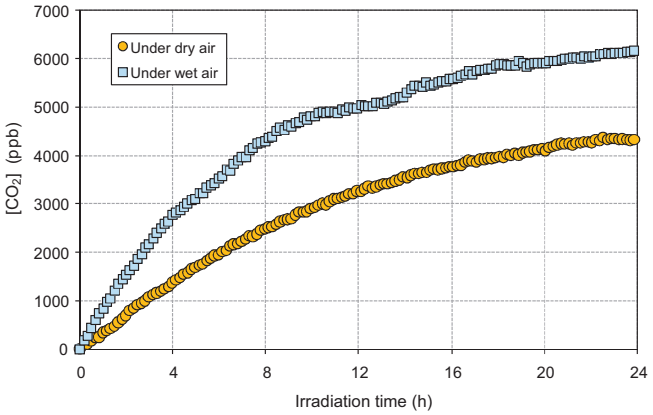

Fig. 16. Change in CO_2 concentration during photocatalytic oxidation of 800 ppb of decane under dry and wet (50% RH) conditions as a function of irradiation time.

presented in the next paragraph, will orient this discussion on the effect of humidity.

3.5. Mineralization of decane into CO and CO_2

3.5.1. Formation of CO_2

In order to determine the fraction of mineralized decane, the concentrations of CO and CO_2 were monitored during the degradation of 800 ppb of decane. Aimed at investigating the influence of relative humidity, this monitoring was performed with both dry and wet air.

The change in CO_2 concentration during the photocatalytic oxidation of 800 ppb of decane under dry and wet conditions is presented in Fig. 16. Irrespective of the humidity level, CO_2 formation starts at the beginning of UV irradiation and tends to stabilize over 20 h. Considering only CO_2, the percentage of mineralization of decane reaches 86% and 59% under wet and dry conditions, respectively. Thus, mineralization is not complete and several reaction intermediates are not totally oxidized. Moreover, as previously reported for toluene PCO at ppb level [4], in the presence of 50% RH, CO_2 concentrations are higher than under dry air conditions during the whole experiment. This is consistent with the first hypothesis proposed in Section 3.4 for the effect of water vapor on reaction intermediate quantities. Mineralization would be promoted by hydroxyl radicals. Decane consumes $HO^\bullet$ from the TiO_2 surface, initially present in the reactor. Thus, moisture does not significantly improve decane consumption. Reaction intermediates immediately formed after decane removal, e.g. decanols, decanones, decenes, stay adsorbed on the TiO_2 surface. They are degraded by hydroxyl radicals under wet air whereas, under dry air, they are less able to react because of the lower $HO^\bullet$ concentration, thus decreasing the percentage of mineralization. Water vapor and $HO^\bullet$ would therefore be crucial elements for the improved mineralization of VOCs by photocatalytic oxidation.

The change in CO concentration during the PCO of 800 ppb of decane is presented in Fig. 16 under dry and wet (50% RH) conditions. Similarly to CO_2, the concentration of CO increases as soon as UV illumination begins and is characterized by an asymptotic behavior. Rosseler has shown that the photocatalytic conversion from CO to CO_2 is possible only if the TiO_2 surface contains oxygen defects [46]. In our case, the surface of TiO_2 P25 is exposed to O_2 and from 10 to 15,500 ppm of water molecules and thus the TiO_2 surface remains stoichiometric. Therefore, CO is not photocatalytically oxidized into CO_2 and can be considered a reaction by-product. Like CO_2, CO formation is promoted by the presence of moisture in the exposure chamber. As discussed in Section 3.3, CO may be

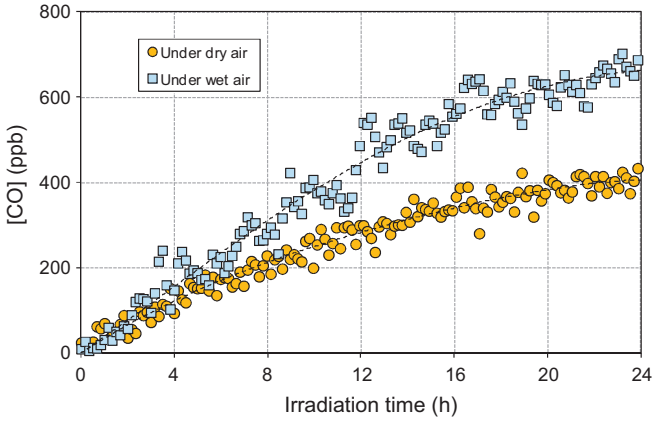

Fig. 17. Change in CO concentration during photocatalytic oxidation of 800 ppb of decane under dry and wet (50% RH) conditions as a function of irradiation time.

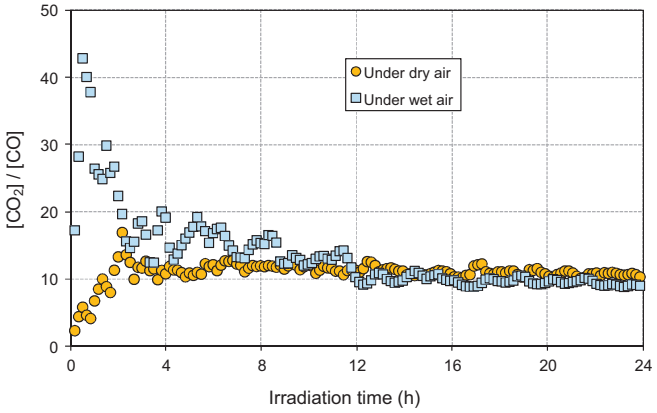

Fig. 18. Change in the $[CO_2]/[CO]$ ratio during the photocatalytic oxidation of 800 ppb of decane under dry (10 ppm H_2O) and wet (13,000 ppm H_2O) air as a function of irradiation time.

preferentially obtained from the oxidation of formates or, more generally, carboxylates (Fig. 17).

Although the temporal profiles of CO and CO_2 follow similar tendencies, Fig. 18 highlights that the concentrations of these two species are not proportional throughout the illumination. Under both dry and wet air, more than 10 h of irradiation are necessary to reach a constant ratio of 10. Of course, the ratio between CO_2 and CO will be highly dependent on the primary compound and its oxidation pathway. In the case of acetylene, Thévenet et al. have calculated a ratio of 25 during the photocatalytic reaction [47]. However, in the case of heptane PCO, Shang et al. reported a ratio of 250 [16]. Moreover, this ratio increased with time until the total elimination of CO. The initial VOC concentration range and, above all, the photocatalytic reactor configuration may also play a significant role in mineralization selectivity.

Before reaching the value of 10, the ratio of $[CO_2]/[CO]$ shows opposing behavior depending on the humidity level. In the presence of dry air, the ratio starts almost from 1 and tends toward 10 within 3 h. This situation indicates that, at the beginning of the reaction, the selectivity toward CO is significant. On the contrary, under wet conditions, the ratio is higher than 10 during the first 8 h attesting to a very high selectivity toward CO_2. As a consequence, the presence of a relative humidity of 50% during the first hours of

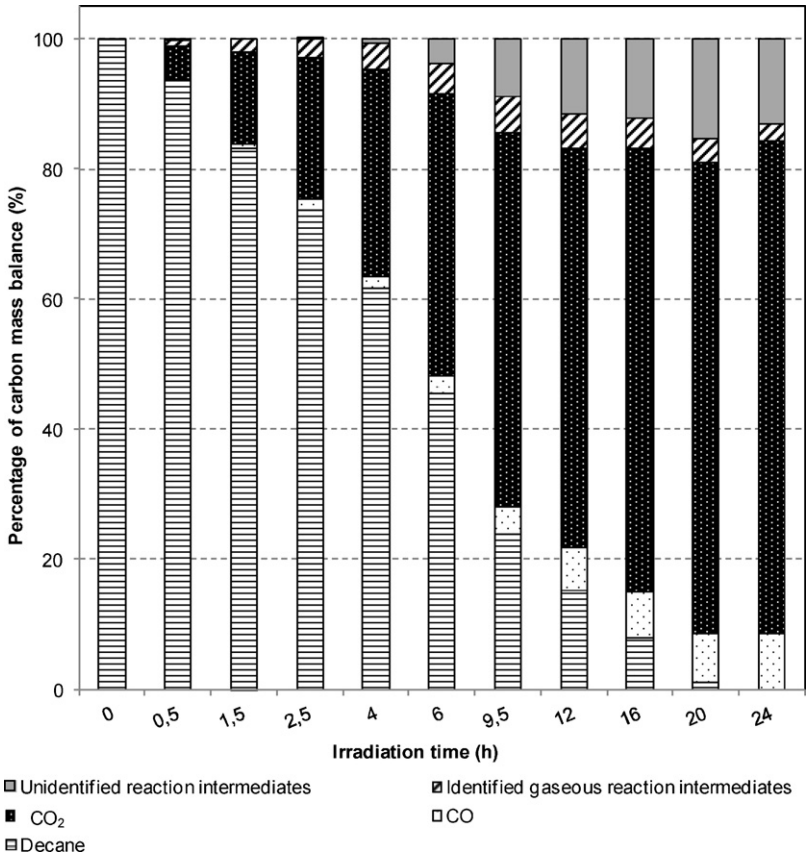

Fig. 19. Contributions of decane, CO, CO_2 and identified and unidentified reaction intermediates to the carbon mass balance of the photocatalytic oxidation of decane for several irradiation times. $C_0^{dec} = 800$ ppb, RH = 50%.

degradation clearly ensures a particularly high selectivity toward CO_2 at the expense of CO.

3.5.2. Carbon mass balance analysis

Using the concentrations of decane, CO, CO_2 and gaseous reaction intermediates, a carbon mass balance of the photocatalytic degradation of 800 ppb of decane under wet air was calculated. The contribution of each compound category in the carbon mass balance was determined and is reported in Fig. 19 as a function of irradiation time. The missing part of the carbon balance is displayed in gray on the graph and labeled as 'unidentified reaction intermediates'. Several points can be highlighted in Fig. 19:

(i) After 24 h of irradiation, the contribution of CO reaches 9%. It is therefore a significant by-product in the photocatalytic degradation of decane at the ppb level.
(ii) The constant increase in the contribution of CO_2 to the carbon mass balance indicates that decane is continuously mineralized. CO_2 represents over 75% of carbon when decane is completely removed from the gas phase. This value is significantly higher than that obtained when toluene was converted under similar conditions (i.e. 45%) [4].
(iii) The contribution of identified reaction intermediates in the gas phase remains lower than 5% of the carbon mass balance. From an indoor air point of view, this result must be highlighted since the release of intermediates in the gas phase compared to the initial amount of pollutant is minor.
(iv) Reaction intermediates that are not detected in the gas phase probably remain adsorbed onto the TiO_2 surface. The maximum contribution of unidentified intermediates to the decane PCO carbon mass balance is 16%. This value is significantly lower than that obtained by Debono et al. for toluene under similar conditions (i.e. 60%) [4]. The aliphatic nature of decane and its reaction intermediates promotes their fast degradation, in comparison with aromatic structures in the case of toluene [48].

4. Conclusion

The photocatalytic oxidation of decane at ppb levels was investigated in a batch reactor under two conditions of relative humidity. A complete characterization of the gas phase throughout the photocatalytic process was carried out by monitoring decane concentrations as well as reaction intermediates, CO and CO_2 concentrations. Our investigations prove that photocatalytic oxidation is effective for eliminating decane at ppb levels as a complete degradation of decane was obtained.

From an air treatment point of view, it was necessary to investigate precisely the gaseous reaction intermediates since they are highlighted as one of the major drawbacks of photocatalytic treatment. 18 reaction intermediates were identified and quantified during decane PCO. Aldehydes were the main reaction intermediates in terms of concentration in the gas phase. The quantities of these intermediates were highly dependent on the experimental conditions such as the irradiation time, the initial decane concentration and the humidity. In order to describe the overall process of decane PCO, a reaction pathway was proposed and the main conclusions regarding the formation of reaction intermediates are the following:

(i) The higher the initial decane concentration is, the more the intermediates are produced.
(ii) Compared to dry conditions, 50% relative humidity tends to increase the concentration of reaction intermediates in the gas phase.
(iii) Reaction intermediates monitored in the gas phase represent no more than 5% of the total carbon mass balance.
(iv) In spite of their diversity, the fraction represented by the reaction intermediates in the carbon balance is very limited in comparison with the primary pollutant. Moreover, only reaction intermediates characterized by the lowest molecular weight reach concentrations that could be significant in indoor air: ethanol, propanal, acetaldehyde, and formaldehyde. The fact that these compounds are clearly identified makes it possible to implement appropriate air treatment systems to avoid their formation or release.

The determination of the mineralization of decane at the ppb level proved that PCO is operational for typical indoor air levels of VOCs. Moreover, measurement of the CO and CO_2 quantities produced is the only way to assess clearly the efficiency of PCO. This study proved that, although the quantification of reaction intermediates and the determination of a carbon mass balance are challenging tasks, they can be achieved at the ppb level and give an overview of PCO efficiency close to real indoor air conditions. The determination of the adsorbed reaction intermediates would consolidate the reaction pathway proposed in this work. From an air treatment point of view, low concentrations of primary pollutant as well as moisture in the air to be treated are favorable conditions for VOC removal and mineralization. Further investigations with other VOCs or mixtures of VOCs would be interesting in order to assess their effects.

Acknowledgments

The authors thank Thierry LEONARDIS and Isabelle FRONVAL, for their valuable technical assistance and the Institut Carnot Mines for financial support.

References

[1] E. Gallego, X. Roca, J.F. Perales, X. Guardino, Determining indoor air quality and identifying the origin of odour episodes in indoor environments, Journal of Environmental Sciences 21 (2009) 333–339.
[2] N. Shinohara, Y. Kai, A. Mizukoshi, M. Fujii, K. Kumagai, Y. Okuizumi, M. Jona, Y. Yanagisawa, On-site passive flux sampler measurement of emission rates of carbonyls and VOCs from multiple indoor sources, Building and Environment 44 (2009) 859–863.
[3] M. Sleiman, P. Conchon, C. Ferronato, J.-M. Chovelon, Photocatalytic oxidation of toluene at indoor air levels (ppbv): towards a better assessment of conversion, reaction intermediates and mineralization, Applied Catalysis B: Environmental 86 (2009) 159–165.
[4] O. Debono, F. Thevenet, P. Gravejat, V. Hequet, C. Raillard, L. Lecoq, N. Locoge, Toluene photocatalytic oxidation at ppbv levels: kinetic investigation and carbon balance determination, Applied Catalysis B: Environmental 106 (2011) 600–608.
[5] N. Djeghri, S.J. Teichner, Heterogeneous photocatalysis: the photooxidation of 2-methylbutane, Journal of Catalysis 62 (1980) 99–106.
[6] T.M. Twesme, D.T. Tompkins, M.A. Anderson, T.W. Root, Photocatalytic oxidation of low molecular weight alkanes: observations with ZrO_2–TiO_2 supported thin films, Applied Catalysis B: Environmental 64 (2006) 153–160.
[7] A.T. Hodgson, H. Levin, Volatile Organic Compounds in Indoor Air: A Review of Concentrations Measured in North America Since 1990, Lawrence Berkeley National Laboratory, 2003, LBNL-51715.
[8] T. Tanaka-Kagawa, S. Uchiyama, E. Matsushima, A. Sasaki, H. Kobayashi, M. Yagi, M. Tsuno, M. Arao, K. Ikemoto, M. Yamasaki, A. Nakashima, Y. Shimizu, Y. Otsubo, M. Ando, H. Jinno, H. Tokunaga, Survey of volatile organic compounds found in indoor and outdoor air samples from Japan, Kokuritsu Iyakuhin Shokuhin Eisei Kenkyujo Hokoku 123 (2005) 27–31.
[9] AFNOR XP B44-013 Standard, Photocatalysis: Test and Analysis Method for Determining the Efficacy of Photocatalytic Systems for Eliminating Volatile Organic Compounds/Odours in Recirculating Interior Air – Confined Chamber Test, 2009.
[10] R. Nakamura, S. Sato, Oxygen species active for photooxidation of n-decane over TiO_2 surfaces, The Journal of Physical Chemistry B 106 (2002) 5893–5896.
[11] W. Balcerski, S.Y. Ryu, M.R. Hoffmann, Gas-phase photodegradation of decane and methanol on TiO_2: dynamic surface chemistry characterized by diffuse reflectance FTIR, International Journal of Photoenergy 2008 (2008).
[12] W. Chen, J. Zhang, Photocatalytic oxidation of multi-component systems an investigation using toluene/ethylbenzene, octane/decane/dodecane and

formaldehyde/acetaldehyde, Journal of Advanced Oxidation Technologies 11 (2008) 163–173.
[13] A.K. Boulamanti, C.J. Philippopoulos, Photocatalytic degradation of C_5–C_7 alkanes in the gas-phase, Atmospheric Environment 43 (2009) 3168–3174.
[14] N. Djeghri, M. Formenti, F. Juillet, S.J. Teichner, Photointeraction on the surface of titanium dioxide between oxygen and alkanes, Faraday Discussions of the Chemical Society 58 (1974) 185–193.
[15] C. Hägglund, B. Kasemo, L. Österlund, In situ reactivity and FTIR study of the wet and dry photooxidation of propane on anatase TiO_2, The Journal of Physical Chemistry B 109 (2005) 10886–10895.
[16] J. Shang, Y. Du, Z. Xu, Photocatalytic oxidation of heptane in the gas-phase over TiO_2, Chemosphere 46 (2002) 93–99.
[17] P. Zhang, J. Liu, Photocatalytic degradation of trace hexane in the gas phase with and without ozone addition: kinetic study, Journal of Photochemistry and Photobiology A: Chemistry 167 (2004) 87–94.
[18] C.F.H. Allen, Journal of American Society 52 (1930) 2955.
[19] P. Coddeville, N. Locoge, J.C. Galloo, Determination of organic compound levels at Donon station, Mera Report, Ecole des Mines de Douai, France, 1998.
[20] C. Raillard, V. Héquet, P.L. Cloirec, J. Legrand, TiO_2 coating types influencing the role of water vapor on the photocatalytic oxidation of methyl ethyl ketone in the gas phase, Applied Catalysis B: Environmental 59 (2005) 213–220.
[21] C. Raillard, V. Héquet, P. Le Cloirec, J. Legrand, Kinetic study of ketones photocatalytic oxidation in gas phase using TiO_2-containing paper: effect of water vapor, Journal of Photochemistry and Photobiology A: Chemistry 163 (2004) 425–431.
[22] C. Raillard, V. Héquet, P. Le Cloirec, J. Legrand, Photocatalytic oxidation of methyl ethyl ketone over sol–gel and commercial TiO_2 for the improvement of indoor air, Water Science & Technology 53 (2006) 107–115.
[23] M.L. Sauer, D.F. Ollis, Photocatalyzed oxidation of ethanol and acetaldehyde in humidified air, Journal of Catalysis 158 (1996) 570.
[24] V. Augugliaro, S. Coluccia, V. Loddo, L. Marchese, G. Martra, L. Palmisano, M. Schiavello, Photocatalytic oxidation of gaseous toluene on anatase TiO_2 catalyst: mechanistic aspects and FT-IR investigation, Applied Catalysis B: Environmental 20 (1999) 15.
[25] J. Peral, D.F. Ollis, Heterogeneous photocatalytic oxidation of gas-phase organics for air purification: acetone, 1-butanol, butyraldehyde, formaldehyde, and m-xylene oxidation, Journal of Catalysis 136 (1992) 554–565.
[26] J.M. Coronado, S. Kataoka, I. Tejedor-Tejedor, M.A. Anderson, Dynamic phenomena during the photocatalytic oxidation of ethanol and acetone over nanocrystalline TiO_2: simultaneous FTIR analysis of gas and surface species, Journal of Catalysis 219 (2003) 219–230.
[27] G. Vincent, P.M. Marquaire, O. Zahraa, Abatement of volatile organic compounds using an annular photocatalytic reactor: study of gaseous acetone, Journal of Photochemistry and Photobiology A: Chemistry 197 (2008) 177–189.
[28] M.A. Henderson, Ethyl radical ejection during photodecomposition of butanone on TiO_2(1 1 0), Surface Science 602 (2008) 3188–3193.
[29] G. Vincent, A. Queffeulou, P.M. Marquaire, O. Zahraa, Remediation of olfactory pollution by photocatalytic degradation process: study of methyl ethyl ketone (MEK), Journal of Photochemistry and Photobiology A: Chemistry 191 (2007) 42–50.
[30] M.D. Hernández-Alonso, I. Tejedor-Tejedor, J.M. Coronado, M.A. Anderson, J. Soria, Operando FTIR study of the photocatalytic oxidation of acetone in air over TiO_2–ZrO_2 thin films, Catalysis Today 143 (2009) 364–373.
[31] A. Mattsson, L. Osterlund, Adsorption and photoinduced decomposition of acetone and acetic acid on anatase, brookite, and rutile TiO_2 nanoparticles, The Journal of Physical Chemistry C 114 (2010) 14121–14132.
[32] W. Xu, D. Raftery, In situ solid-state nuclear magnetic resonance studies of acetone photocatalytic oxidation on titanium oxide surfaces, Journal of Catalysis 204 (2001) 110–117.
[33] M.A. Henderson, Effect of coadsorbed water on the photodecomposition of acetone on TiO_2(1 1 0), Journal of Catalysis 256 (2008) 287–292.
[34] A.L. Attwood, J.L. Edwards, C.C. Rowlands, D.M. Murphy, Identification of a surface alkylperoxy radical in the photocatalytic oxidation of acetone/O_2 over TiO_2, The Journal of Physical Chemistry A 107 (2003) 1779–1782.
[35] E. Piera, J.A. Ayllón, X. Doménech, J. Peral, TiO_2 deactivation during gas-phase photocatalytic oxidation of ethanol, Catalysis Today 76 (2002) 259–270.
[36] T. Ohno, Y. Masaki, S. Hirayama, M. Matsumura, TiO_2-photocatalyzed epoxidation of 1-decene by H_2O_2 under visible light, Journal of Catalysis 204 (2001) 163–168.
[37] E. Obuchi, T. Sakamoto, K. Nakano, F. Shiraishi, Photocatalytic decomposition of acetaldehyde over TiO_2/SiO_2 catalyst, Chemical Engineering Science 54 (1999) 1525–1530.
[38] I. Sopyan, M. Watanabe, S. Murasawa, K. Hashimoto, A. Fujishima, An efficient TiO_2 thin-film photocatalyst: photocatalytic properties in gas-phase acetaldehyde degradation, Journal of Photochemistry and Photobiology A: Chemistry 98 (1996) 79–86.
[39] X. Ye, D. Chen, J. Gossage, K. Li, Photocatalytic oxidation of aldehydes: byproduct identification and reaction pathway, Journal of Photochemistry and Photobiology A: Chemistry 183 (2006) 35–40.
[40] R. Méndez-Roman, N. Cardona-Martinez, Relationship between the formation of surface species and catalyst deactivation during the gas-phase photocatalytic oxidation of toluene, Catalysis Today 40 (1998) 353–365.
[41] P.-A. Deveau, F. Arsac, P.-X. Thivel, C. Ferronato, F. Delpech, J.-M. Chovelon, P. Kaluzny, C. Monnet, Different methods in TiO_2 photodegradation mechanism studies: gaseous and TiO_2-adsorbed phases, Journal of Hazardous Materials 144 (2007) 692–697.
[42] H. Kominami, H. Sugahara, K. Hashimoto, Photocatalytic selective oxidation of methanol to methyl formate in gas phase over titanium(IV) oxide in a flow-type reactor, Catalysis Communications 11 (2010) 426–429.
[43] M.C. Blount, D.H. Kim, J.L. Falconer, Transparent thin-film TiO_2 photocatalysts with high activity, Environmental Science & Technology 35 (2001) 2988–2994.
[44] J. Mo, Y. Zhang, Q. Xu, Y. Zhu, J.J. Lamson, R. Zhao, Determination and risk assessment of by-products resulting from photocatalytic oxidation of toluene, Applied Catalysis B: Environmental 89 (2009) 570.
[45] D.S. Muggli, J.L. Falconer, Parallel pathways for photocatalytic decomposition of acetic acid on TiO_2, Journal of Catalysis 187 (1999) 230–237.
[46] O. Rosseler, Depollution and decontamination of air in indoor environments by photocatalytic oxidation, Ph.D. Thesis, Université de Strasbourg, France, 2010.
[47] F. Thévenet, O. Guaitella, E. Puzenat, C. Guillard, A. Rousseau, Influence of water vapour on plasma/photocatalytic oxidation efficiency of acetylene, Applied Catalysis B: Environmental 84 (2008) 813–820.
[48] R.M. Alberici, W.F. Jardim, Photocatalytic destruction of VOCs in the gas-phase using titanium dioxide, Applied Catalysis B: Environmental 14 (1997) 55–68.